STUDY OF TWO-DIMENSIONAL CALCULATIONS OF CRATERING

PIFR-101

FINAL REPORT
March 30, 1964

Prepared for National Aeronautics & Space Administration
Goddard Space Flight Center
Greenbelt, Maryland

BY

Charles S. Godfrey Dudley J. Andrews Richard D. Levee
Physics International Company
2229 Fourth Street
Berkeley, California

Under Contract No. NAS 5-3110

ABSTRACT

The development of a calculational program, whose goal is to predict the response of earth media to the impact of a hypervelocity projectile, is described. A vital part of the program has involved the derivation of calculational models capable of describing the response of earth media to shock loading. A test problem involving the impact of an iron cylinder on an aluminum half-plane at a velocity of 3 cm/μsec has been run on the two-dimensional plastic-elastic time-dependent code, PIPE. Results, conclusions and recommendations are given.

TABLE OF CONTENTS

SECTION 5

SECTION 6

LIST OF ILLUSTRATIONS

SECTION 1

INTRODUCTION

1.1 Statement of the Problem

During the past few years a great amount of attention has been focused on crater formation on the earth and the moon by meteoritic impact. Craters on earth which show evidence of meteoritic origin have been investigated and in many cases their internal structure has been determined in some detail.[1, 2] Explosion craters and scaling laws have been used generally to indicate the depth of burial and energy required to produce a crater of a given diameter and depth. Applications have been to both earth and lunar craters.[2] Such applications involve the assumption that hypervelocity meteorites vaporize upon impact and that the explosive expansion of the vapor produces the resultant crater.

In fact, however, impact cratering and explosive cratering differ in two important ways; in the partition of energy between internal and kinetic and in the geometry of the energy distribution. In impact cratering all energy is kinetic and is delivered as a line source. In explosive cratering the energy is divided between internal and kinetic and is distributed over a roughly spherical volume. Thus, descriptions of the structure of an impact crater which derive from explosive cratering are likely to be in considerable error.

The basic physics of earth and lunar crater formation can best be understood by theoretical calculations. Such calculations involve the development of a computer code which follows the detailed flow of material and energy partition as a function of time in two space dimensions, once the target and projectile characteristics have been specified. Although material strength is not important in the early phases, it must be included in the later phases in order to properly describe the crater formation.

A vital part of a crater calculation lies in selecting adequate mathematical descriptions of the earth media when subject to dynamic loading. In particular, elastic deformation, plastic yielding and compaction must be taken into account.

1.2 Survey of Previous Work

The problem of crater formation by hypervelocity impact has received extensive treatment by experimentalists. However, most of this work has been on metal-metal impacts. A review of the state-of-the-art has been made recently by Bjork.[3] Metal projectile impacts on soil-like targets have been sadly lacking. One experiment, on the impact of steel into Coconino sandstone, is reported by Moore et al.[4]

Theoretically, the situation with regard to calculations of metal impact on soil is not appreciably better. A preliminary report on the formation of the Arizona meteor crater is given by Bjork.[5] His calculations assumed the process was purely hydrodynamic. Such a treatment is satisfactory for pressures greater than a few hundred kilobars. Below these pressures, material strength becomes important in arresting the flow and should be included. His calculations were for the impact of an iron meteorite into tuff since the equations of state of limestone and sandstone (the actual materials of the Arizona meteor crater region) were not available. Theoretical calculations of metal on metal impact are reported by Walsh and Tillotson.[6] Here again, material strength was not included.

Several two-dimensional time-dependent calculational codes embodying a plastic-elastic description of matter have been developed. Of these, TENSOR,[7] although designed specifically for calculation of cratering, was never made operational. PICKWICK[8] had not yet included the strength of materials in its applications when last reported.

HEMP[9] has been used successfully to investigate problems involving the interaction of high explosive energy sources with metals. Although not designed specifically for cratering, it seemed to offer the most advanced and most logical starting place for the development of a two-dimensional time-dependent plastic-elastic calculational code for impact cratering.

The conclusions of various investigators may be summed up as follows:

1. Hypervelocity impact cratering is not an explosive phenomena.
2. Material strength cannot be ignored.
3. The equation of state of the soil media must be fairly well established.
4. Detailed computer codes which follow the detailed motions of the material, such as throwout, fall-back and lip formation, and of the ground shock are capable of leading to a understanding of crater formation.
5. Experiments of metal on soil impacts are a necessary link to the theoretical codes.
6. Existing craters should be thoroughly analyzed with the computer code.

SECTION 2
DESCRIPTION OF HEMP CODE

2.1 General

HEMP[9] is a code which was developed by Mark Wilkins and Richard Giroux at the University of California, Lawrence Radiation Laboratory, Livermore. It is written in machine language for the IBM Stretch. The reference gives a very complete description of the code. Since it represents a point of departure for our code, PIPE, a brief description of its features is appropriate here.

2.2 Elastic Region

Basically, HEMP is a two-dimensional time-dependent hydrodynamic calculational code to which has been added an equation of state capable of describing elastic and elastic-plastic flow. During the elastic phase, the material is assumed to follow Hooke's Law. The stresses are decomposed into a hydrostatic component P (all three stress components equal) and an anistropic component s (stress deviator) which describes the resistance of the material to shear distortion. These deviators are defined in such a way that

$$s_1 + s_2 + s_3 = 0 \qquad (1)$$

where s_1, s_2, and s_3 are the principal stress deviators. The stress deviators are calculated in terms of an incremental stress resulting from an incremental strain. Hooke's Law used in this way gives natural strain, which means that the strain of an element is referred to the current configuration instead of the original configuration.

2.3 Yield Condition and Plastic Flow

Most yield criteria postulate some relation between the principal stresses as a condition for yielding. Since the code calculates the principal stresses at every element for every time step, it is possible to incorporate any such criterion into the code and test each element at each time step to determine whether or not the elastic limit has been reached. In the current version of HEMP, the yield condition of R. Von Mises is used to describe the elastic limit. When the principal stresses are known, the yield condition can be written as:

$$(\sigma_1 - \sigma_2)^2 + (\sigma_2 - \sigma_3)^2 + (\sigma_3 - \sigma_1)^2 = 2(y^o)^2 \qquad (2)$$

where σ_1, σ_2, σ_3 are the principal stresses and
y^o is the yield strength in simple tension.

The left side of this expression is proportional to the elastic energy of distortion per unit volume or the energy required to change shape as opposed to the energy that causes a volume change. The expression states, therefore, that plastic flow begins when the elastic distortion energy reaches a limiting value and that this energy remains constant during the plastic flow. Thus, by the term "elastic-plastic" is meant the state whereby the distortion (change in shape) component of the strained material has been loaded, following Hooke's Law, up to a state where the material can no longer store elastic energy. All subsequent distortion will produce plastic flow and plastic work will be done.

Since pressure is common to all stresses of Equation (2), the equation can be written as

$$(s_1 - s_2)^2 + (s_2 - s_3)^2 + (s_3 - s_1)^2 = 2(y^o)^2 \qquad (3)$$

Equations (1) and (3) can be combined to give

$$s_1^2 + s_2^2 + s_3^2 \leq \frac{2}{3} (y^\circ)^2 \qquad (4)$$

The inequality defines the elastic region in which the element in question is still behaving elastically. The equality indicates the condition at the onset of plastic flow and the condition which is maintained during plastic flow. If an incremental change in the stresses of an element result in the left hand side of Equation (4) exceeding the right hand side, then each of the principal stress deviators (s_1, s_2, and s_3) are adjusted such that Equation (4) is again satisfied.

The above formulation corresponds to a perfectly plastic material, i.e., material that flows plastically under a constant stress without work-hardening. For a work-hardening material the stress will increase monotonically with strain for strains beyond the yield point instead of remaining constant as for a perfectly plastic material. Work-hardening can be introduced into the calculation by making the constant y° in Equation (2) a function of the strain energy, for example. Also, when enough work has been done to melt the material, the value of y° can be set to zero. In this way an all-hydrodynamic description will follow since the stress deviators will automatically be set to zero by the above procedure and the only remaining stress will be the pressure P. Time-dependent yielding can be macroscopically represented by selecting a high yield constant y° if the strain rates ($\dot{\epsilon}_1$, $\dot{\epsilon}_2$, $\dot{\epsilon}_3$) are above some prescribed value.

2.4 Other Features

The other features of the code are briefly summarized. The code employs a Lagrangian coordinate system which moves with the material. A routine exists for the detonation and subsequent burning of high explosive. Sliding interfaces are allowed between an elastic

and a hydrodynamic region, but not between two elastic boundaries. An elastic region, however, may slide along a fixed boundary. An artificial viscosity (q) is used to provide stability in the region of a shock. Three alternate forms of q are available; a linear q, a quadratic q, and an anistropic q. The latter is useful for problems where a shock is traveling perpendicular to a free surface. The specification of an equation of state for a material used in the code requires the usual relation of pressure as a function of relative volume and internal energy. In addition one must specify Y° and the shear modulus of the material (μ).

SECTION 3
DESCRIPTION OF PIPE CODE

3.1 Machine Language PIPE Code

PIPE is the designation of the Physics International Plastic-Elastic Code. This code uses the same basic equations as HEMP, but is coded to run on an IBM 7094. One of the first problems that had to be faced was providing sufficient number of zones to perform a cratering problem. It was recognized from one-dimensional calculations that a large number of zones would be required to retain the structure of a shock, particularly in lower pressure regions where the shock structure can be quite complex. Since the code must retain 21 quantities in memory for each zone, the problem can be readily visualized. By using intermediate tape storage, it was possible to provide for 120 zones in one direction and an unlimited number in the other.

The intermediate storage makes use of four tape units for maximum efficiency. Half the zones are read from Tape 1 while being written on Tape 2. The second half are read from Tape 3 while being written on Tape 4. This latter step allows Tapes 1 and 2 to be rewound while computation is going on. Thus, Tapes 1 and 2 are in position for the next time step when Tapes 3 and 4 have been read and written completely.

Another problem which was known at the outset was the limitation of a Lagrangian code for problems in which a large distortion of the zones takes place. Examples of such distortions are shown in Section 5. It was hoped, however, that by the use of a rezone routine reasonable orthogonality could be maintained. Consequently, a routine was desired which could remap a distorted grid into a new, more orthogonal, grid.

The first step needed was a plot routine to map the grid at any desired time. Since Physics International personnel planned on using the Cal Comp plotter of the IBM Service Bureau Corporation, it was convenient to use the 1401 FORTRAN plotting routines which had been designed for this plotter. This required routines to write an output tape which could be read by the FORTRAN plotting routines. The present routine only plots the two-dimensional configuration. Sample plots are shown in Section 5. The plot can be magnified to show any degree of detail for any desired region of the grid.

The next logical step in a rezone procedure would be an automatic remapping routine. To provide automatic rezoning requires a routine to test the grid periodically for orthogonality and take corrective action. It is conceivable that a grid could be made to rezone itself periodically in such a way that some degree of orthogonality would be maintained. We do not see any practical way of providing such a feature in the existing code. It is possible that a combined Eulerian-Lagrangian code would better fulfill this function.

The next best to an automatic routine was determined to be one where a knowledgeable human remaps the problem on the Cal Comp plot by sketching in a new desired grid. The coordinates of the new boundary points are then read off and serve as input to the rezone calculation. Up to 100 points at a time can be rezoned. All points on the boundaries of the region to be rezoned must be specified. The positions, velocities, relative volume, energy, pressure and stress deviators are determined for the new zones. The number of new zones is always equal to the number of old zones. The routine conserves mass, energy and momentum to at least first order.

SECTION 4
EQUATION OF STATE OF EARTH MEDIA

4.1 General

This contract required that Physics International incorporate into PIPE a model appropriate for the description calculations of earth media when subjected to dynamic loading. An intensive effort has been sponsored by AFWL (see, for example, Reference 10) to determine reliable equations of state for earth materials under extremely high pressures and rapid loading rates. This effort has been both experimental and theoretical. "Equation of state" in this context is not simply the shock Hugoniot curve, but includes consideration of a non-isotropic stress tensor.

4.2 Experimental Data

Measurements of the static and dynamic behavior of playa in one-dimensional compression have been made.[11] Some Hugoniot data for playa also exists.[12, 13] The stresses attained in Reference (11) were limited to ≤1.4 kilobar and the time of application of this stress to ≥3 milliseconds. The Hugoniot data covers a pressure region from 40 to 270 kilobars and moisture contents from 0 to 10%. Therefore, no data exist in the pressure region from 1.4 to 40 kilobars, and no data with realistic dynamic loading times exist below 40 kilobars.

More complete data exist for some other earth media.[14, 15, 16, 17, 18] S.R.I., for example, has measured Hugoniot data in the pressure range 5 to 250 kilobars for quartzite,

sandstone, calcite, marble, limestone, plagiodase and basalt. Work on other media continues. The recent development of pressure transducers capable of recording pressure as a function of time in dynamically loaded samples[19] promises to provide a new dimension to the acquisition of equation of state data. With such transducers, the elastic and plastic loading and unloading characteristics of a sample can be investigated. From this information will come sufficient insight to develop rather sophisticated equation of state models to describe the behavior of earth media.

4.3 Physical Description of An Earth Medium

A typical earth medium is a mixture of mineral particles, water, and air. The mineral particles can be considered to be cemented together to form a porous skeleton, the pores of which are filled with water and air. For sufficiently small loadings, the rigidity of the skeleton will resist deformation in an elastic manner. Under increasing load, however, the skeleton will gradually break up. The mineral particles will be compacted irreversibly, the porosity will decrease and a larger fraction of the load will be borne by the water and air. As the load increases farther, the mineral particles themselves will also begin to be fractured as they are forced into more and more intimate contact with their neighbors. It is apparent that the above compaction is irreversible, and that a reduction of load at this point will bring about a very small increase in volume compared to the large decrease in volume during loading. The complete breakdown of the skeleton, in fact, destroys any knowledge the system might have had concerning its initial condition. As the load becomes even larger, the compacted mixture can eventually be treated as a fluid whose density is a unique function of the mean pressure for an adiabatic compression or expansion.

When earth media are subjected to shock or wave motion, it is necessary to account for significant energy absorption, even at small stresses. Field measurements on contained explosions at ranges where spherical symmetry should apply have generally indicated that peak stress and particle velocity are proportional to $R^{-\alpha}$ where α is always larger than one and is usually larger than two. Such a dependence has been observed at ranges large enough that the particle velocity is much less than the shock velocity, so that the acoustic limit is approached. But in a non-dissipative medium in the acoustic limit, the amplitude of a spherical pulse is proportional to R^{-1}. Therefore, the measurements do not indicate any stress level below which dissipation is unimportant. To predict the observed attenuation, a model of the material must be used which allows irreversible processes at low stresses.

The effect of several types of irreversibility may be discussed qualitatively. The first arises from the increase in entropy upon shock loading, which is important for strong shocks. At small stresses the Hugoniot is equal to the adiabat to third order, so that irreversibility of this type becomes less important.

A second type is plastic yielding, an irreversible change of shape. If the yield stress is independent of pressure, then beyond a certain radius the wave will be elastic and no more energy will be lost to this mechanism. The case in which the yield stress is proportional to pressure, as derived from Coulomb friction, warrants further study.

A third type is comminution, irreversible change of volume. This process will take place in porous materials. Experiments have indicated that the ratio of the energy absorbed to the energy of loading of a sample does not approach zero at small stresses.

(The model used in the work reported here has this feature.) Therefore, comminution will contribute to attenuation at all stress levels, and could explain the attenuation observed in porous media. But it cannot be the only energy sink operative at small stresses, because attenuation has been observed in non-porous materials such as granite.

Other possible mechanisms of energy absorption would arise from rate-dependent stresses, such as viscosity. We have not considered such processes. The fact that scaling laws work as well as they do is an argument for neglecting such effects at this stage.

4.4 Model of An Earth Medium

The model proposed here has much in common with that proposed by Grigorian[20, 21, 22] and experimental work done in support of that model.[23, 24] Although such a model is extremely difficult to apply in any analytical fashion, its use in a code such as PIPE becomes a very powerful tool for the understanding of earth shock phenomena.

A model for the change of pressure, as a function of η-1 (where $\eta = \frac{\rho}{\rho_o}$) might logically have the properties of that shown in Figure 4.1a. Here the three load regimes discussed above are represented by the portions of the curve, ab, bd, and de, respectively. It is apparent from the discussion above that the unloading curves will be quite different from this loading curve. As an approximation, the unloading paths from point, c and d, might be represented by the paths, cg, and df, respectively.

When the energy necessary to perform a shear deformation of the material cannot be neglected, one must consider the deforming stress tensor rather than a pressure. As mentioned in Section 2,

it is convenient to consider the stresses as being composed of a mean pressure responsible for the volume deformation and the deviatoric stresses responsible for the shear deformation. To the model shown in Figure 4.1a, therefore, must be added the appropriate description of the stress deviators during elastic and plastic deformation of the body.

In HEMP, this relationship is provided by Hooke's Law in the elastic region and the Von Mises yield criteria in the plastic region. The Von Mises yield criteria has been most sucessfully applied to the plastic yielding of ductile metals. Although Hooke's Law is a sound basis for any elastic behavior, the Von Mises criteria is not necessarily the best that can be applied to an earth media. In fact, it is usually accepted that some form of the Coulomb yield condition is more appropriate.[25] Both forms have been incorporated into our model.

4.4.1 Von Mises Model

In the Von Mises model, the Von Mises criteria is superimposed on the pressure-volume model described above. The slope, ab, is the initial bulk modulus K of the medium. The curve, bcde, is a best fit such that the superposition of the pressure curve with the axial stress deviator produces a total stress curve which matches the stresses measured in one-dimensional experiments. The axial stress deviator (s_1) for one-dimensional loading is shown in Figure 4.1b. A typical unloading path is jk. Figure 4.1c shows the total axial stress (σ_1) formed by a superposition of P and s_1. The slope, lm, is chosen to give the observed sound speed in the medium. In Wilkins' model,[9] y° is the yield stress of a tensile test specimen. In our case this definition has no significance. The yield stress should preferably come from a dynamic measurement. The curve, op, is the normal Hugoniot (the stress deviators are set equal to zero on the Hugoniot). A typical unloading path for σ_1 is shown as nq.

The irreversible work done in the loading-unloading cycle, lmnq, is that done in plastic shear deformation, hijk, plus that done in permanent volumetric compaction, abcg. In the usual two-dimensional problem, the directions and magnitudes of the principal stress deviators are not so obvious and must be obtained from the detailed calculation.

The measured Hugoniot of sandstone[17] is shown in Figure 4.2. It can be seen that our model has a form which is very similar to that observed for this soft porous rock.

4.4.2 Coulomb Model

In the Coulomb Model, it has been convenient to choose a relationship between pressure P and relative volume V such that

$$P = -K \ln V \tag{5}$$

Mohr[26] postulated that, in a granular material, the shear stress in any plane section can never become larger than the friction force caused by the normal pressure in this section when slip starts. Interpreted in terms of Coulomb's Law of friction, which states that the friction force is proportional to the normal force, the limiting condition for slip becomes

$$\sigma_1 - \sigma_3 = (\sigma_1 + \sigma_3) \sin \tan^{-1} \mu \tag{6}$$

where σ_1 and σ_3 are the major and minor compressive, principal stresses, μ is the coefficient of sliding friction between the grain. Since $\frac{\sigma_1 - \sigma_3}{2}$ is the maximum shear stress and $\frac{\sigma_1 + \sigma_3}{2}$ is roughly proportional to the mean stress or pressure, the qualitative statement of the criteria is that the shear stress at failure is proportional to the pressure.

The Coulomb condition can be applied more generally by making the octahedral shearing stress a function of the mean stress (i.e. pressure). In our model we have chosen to make the general yield condition

$$(\sigma_1 - \sigma_2)^2 + (\sigma_2 - \sigma_3)^2 + (\sigma_3 - \sigma_1)^2 = 2(y)^2 \tag{7}$$

where

$$y = y^\circ + aP + bP^2 \tag{8}$$

a and b are constant determined from experimental data.

In terms of the one-dimensional model demonstrated in Figure 4.3, the yield condition is described by the equality in the relation

$$-s_1 \leq \tfrac{2}{3} y \tag{9}$$

As the pressure increases, it takes a correspondingly higher stress to cause plastic flow (i.e. slippage).

The total stress is again a superposition of P and $-s_1$. A typical relaxation path is shown as nq.

The model itself is extremely flexible and can be made to fit a wide range of earth media. Unfortunately, the experimental data available is not yet good enough to make the best use of the capabilities of the model.

4.4.3 Specific Model Used in One-Dimensional Calculations

The available Hugoniot data on geologic materials shows a large scatter of points due to unavoidable non-uniformity of the samples. Also the extrapolation of these data to small stresses is uncertain since the Hugoniot curves have abrupt changes of slope due to plastic yielding and comminution. In order to use a larger number of points for fitting a curve it was decided to develop a composite equation of state for tuff, playa and desert alluvium. It was found that by plotting $\rho_o U^2$ vs US the points could be reconciled and a curve could be fitted. Here is the initial density, U is the particle velocity, and S is the shock velocity (see Figure 4.4). This curve translated to a plot of pressure vs volume gives the curve shown in Figure 4.5 except for the portion below 40 kilobars. A justification of the procedure is that this curve is close to the Hugoniot for quartz and so can be interpreted as representing the compacted material. It is assumed that relaxation from a pressure greater than 40 kilobars will lead to a final relative volume of 0.65. The loading curve at small stresses was required to fit the bulk modulus of tuff. It is shown on an enlarged scale in Figure 4.6 with some typical unloading paths for partially compacted material. The shear modulus used was 0.055 megabars which gives a sound speed of 2.72 meters per millisecond. The yield stress chosen was 1.5 kilobars and was assumed constant (i.e. Von Mises model).

The experimental data used for determining this equation of state are for dry materials. Our fit to the data implies a void fraction of 0.35, and can not be expected to represent materials containing water. It has been found that the compaction has a large effect on the attenuation of shock stress with distance.

The specific model described above was used in all one-dimensional calculations reported herein. We have recently completed a model description of the Coulomb type, but have not yet applied it to any calculations.

SECTION 5

CALCULATIONAL PROGRAM

5.1 One-Dimensional Calculations

The numerical calculations of ground motion and shock propagation have been performed with the equation of state for porous materials discussed in the previous section. A number of one-dimensional problems have been run to provide predictions on contained explosions. Because of the simplicity of calculations in one-dimension, they have also been used to examine the dynamic behavior of a material obeying this equation of state. The essential assumption, of course, is that there is spherical symmetry. Gravitational fields are absent and the earth-like medium is initially homogeneous.

The first calculation attempted to represent the Rainier test in tuff. The nuclear energy source was a uniform sphere of hot gas with a radius of 1.2 meters and a total internal energy of 1.7 kilotons. The most significant result of this calculation is that the irreversible volume change has an important effect on the decrease of shock strength with distance. Our values of pressure and particle velocity are smaller than those calculated by Nuckolls.[27] He used a similar equation of state except that there was no compaction. Therefore, compaction cannot be ignored in a porous medium. However, our results do not agree with the measurements. Evidently the void fraction in the Rainier tuff was smaller than 0.35, as we have assumed, possibly due to pure water. Peak stress is plotted against scaled range in Figure 5.1.

In the second calculation it was assumed that a nuclear device was "tamped"; that is, there was no void between it and the earth-like medium. Again the source was taken to be a sphere of hot gas. Because of the smaller volume, the initial energy density and pressure were higher than in the Rainier case. The resulting peak stress is plotted in Figure 5.1. At equal scaled ranges this curve lies below that for the untamped case, since there is increased energy absorption at small distances. In the same figure, experimental points from Project NOUGAT in alluvium are plotted. The agreement is good, so that our equation of state represents dry alluvium with some confidence at the measured stress levels.

5.2 Definition of the Two-Dimensional Problem

The calculational effort using the two-dimensional PIPE code has been applied to the impact of an iron projectile on an aluminum half plane at a velocity of 3 cm/μsec. The basic assumption is that axial symmetry exists about a line perpendicular to the aluminum surface through the center of impact. The projectile is a right circular cylinder with a mass of 6.15 grams and height and diameter each equal to 1 cm. Its initial velocity is directed along the axis of symmetry.

The equation of state used for the aluminum is a fit to the experimentally determined Hugoniot points. It has an energy dependence such that at high pressures it approaches the Thomas-Fermi equation of state. The elastic-plastic properties are specified by the shear modulus, which was taken from static measurements, and the yield stress, which was chosen to be 10 kilobars. This yield stress is several times larger than is reasonable, but at early stages it helps prevent a sharp crater lip from forming without affecting gross features such as the crater depth as a function of time.

The initial projectile density is equal to that of iron. Since only the high pressure behavior of the projectile is important, it is treated as an ideal monatomic gas. To prevent large distortions at very early times a large linear viscosity is used in the projectile.

5.3 Two-Dimensional Calculation

Before the tape storage feature of PIPE was operational, a calculation with a limited number of zones was attempted. This first attempt was overly ambitious in extending the small number of zones over an area so large that the zone dimensions were not small compared to the projectile. The results had little value and were discarded.

When the tape memory became available another problem was started. The impact velocity and the equation of state were the same as before. Smaller zones were used. The large distortion and flow of material in a cratering problem introduce difficulties into a Lagrange calculation which can not be avoided. The problem was run to 0.215 μsec, when it became necessary to rezone and discard the material in the crater lip. The configuration at this time is shown in Figure 5.2. After rezoning, the problem was continued to 0.230 μsec when another rezone was necessary. The last stage of the problem reached 0.416 μsec.

A portion of the configuration at 0.245 μ sec is shown in Figure 5.3. At this time the penetration is 0.58 cm. The velocity and pressure at the center of the interface between the target and projectile are 2.35 cm/ μsec and 10 megabars respectively. These values have remained constant since the beginning of the problem. A portion of the final configuration at 0.416 μsec is shown in Figure 5.4. Rarefactions from the free surfaces have reduced the interface velocity and pressure to 1.8 cm/ μsec and 7 megabars. The penetration is 0.92 cm. The maximum upward velocity in the crater lip is 5.7 cm/ μsec.

The calculation has been carried through only the very early stages of the impact. One might expect a final penetration of 6 cm, so that the final crater volume would be about 200 times larger than that reached here.

SECTION 6

CONCLUSIONS AND RECOMMENDATIONS

6.1 Conclusions

The basic objective of the program was to develop a code capable of calculating the response of a soil-like media to the hypervelocity impact of a metal projectile.

With this objective in mind, an existing Lagrangian elastic-plastic hydrodynamic code (HEMP) was developed into a code capable of handling cratering problems (PIPE). Substantial effort went into the development of a material behavior model suitable for the description of earth media. Spherically symmetric calculations were made using a one-dimensional plastic-elastic code to determine the response of earth media to several past underground detonations. Although the data available from these experiments are meager, the comparisons were constructive in allowing us to improve our model. The resultant model is considerably more sophisticated than is the dynamic experimental data available to specify the parameters of the model.

The code developed was applied to the calculation of the response of an aluminum half plane to the impact of a 6.15 gram cylindrical iron projectile moving with an initial velocity of 3 cm/μsec. The important conclusion reached from this test problem was that a Lagrangian code has distinct limits in dealing with the highly asymmetric flow of material that occurs in the early stage of cratering. In addition, such a code is not capable of calculating the distribution of the ejected material or of giving a detailed description of the lip formation.

6.2 Recommendations

Although the basic objective of the program has not yet been obtained, the progress made is encouraging enough to warrant a continuation of the program. Therefore, the recommendations which follow apply to a follow-on program and suggest the direction it should take.

6.2.1 The Computational Scheme

The most severe restriction on the use of PIPE is the zone distortion. Several approaches may be used to solve this problem. One is to use an Eulerian code for the initial motion and, at the appropriate time, transfer to a Lagrangian code. A second method is to have a combined Eulerian and Lagrangian code, the motion of whose grid can be programmed to move at velocities between the limits of a stationary grid (pure Eulerian) and a grid moving with the material (pure Lagrangian). A third is to have a Lagrange code which periodically tests the zoning for orthogonality and automatically rezones itself when necessary. A fourth is to develop an Eulerian code having an elastic-plastic description adequate to compute the entire cratering phenomenon. Finally, one might use an Eulerian code for the first phase but transfer to an Eulerian-Lagrangian code for the second phase where the Lagrangian code is used in regions in which no mixing takes place, which are not in violent motion, but in which material strength plays an important role.

The first of these approaches has the disadvantage that ejecta and lip formation cannot be followed in the second phase. The second method may ultimately prove to be a fine technique but such a code requires considerable development and a fairly complete understanding of the type of problem it is to be applied to, since grid velocities must be programmed in. The third method suffers from the

lack of a way to handle ejecta, lip formation and the mixing of air, earth and meteoritic materials. The fourth had the disadvantages of the difficulty encountered in putting in the material strength and of a considerable loss of the details of the ground shock effects. This latter difficulty results from the diffusive properties of Eulerian schemes.

We believe that the last suggested approach has no severe disadvantages for surface detonations. For such problems, Figure 6.1 describes the two phases of calculation. Initially, all regions are purely Eulerian. Violent motions occur in this phase but no problems arise.

After pressures in the ground have decreased to a level where material strength becomes important, the lower region outside the surface ABCDE is allowed to become a Lagrange region. This allows the ground shock to be followed accurately. The region above the Eulerian slip surface, ABCDE, continues to handle ejecta, lip formation fall-back and mixing in an appropriate manner.

As the Lagrangian zones expand somewhat radially from the source point, additional zones will be inserted automatically to control the size of the innermost Lagrangian zone. Also, zones will be deleted automatically as they become unnecessary. It should be noted that no rezoning is necessary when going from the first to the second phase. The Eulerian grid is just switched to a Lagrangian grid in the appropriate region. The boundary ABCDE must of course be treated specially. The zoning is in polar coordinates in both phases.

Since this latter scheme offers a direct approach to an immediate calculational capability by the use of PIC and PIPE, and, since in addition, it is ideally suited to describing all the features of impact cratering, we propose its use for such problems.

6.2.2 Physical Phenomena to be Included

It is important to include spall, the mixing of ground, air and projectile material, and gravity. An Eulerian description for the early phases of the calculation will facilitate the second. The addition of gravity may make it possible to determine the final location of the ejected material and hence, to define the apparent shape of the crater. However, because of the long times involved, a separate routine might be necessary. To allow for surface spall it is necessary to invoke the condition that no tensile stresses greater than the fracture stress can exist.

6.2.3 Experiments

It is recommended that several impacts of iron projectiles on soil-like media be made for future comparison and normalization. The velocities should cover the range from 11 km/sec to 72 km/sec at several angles of incidence. It is also recommended that efforts be increased to determine equations of state data for the earth impact crater materials.

6.2.4 Comparisons

It is recommended that when a production code is completed which is capable of describing the meteorite cratering process, detailed comparisons be made of an explosive cratering calculation for a given explosive energy density and an impact cratering calculation for the same energy density. In addition, calculations should be made on the earth craters for which the internal structure is well known.

REFERENCES

1. Proceedings of the Geophysical Laboratory - Lawrence Radiation Laboratory Cratering Symposium, Papers A, B, C and D, UCRL 6438, Part I, (October, 1961).

2. Baldwin, R. B., "The Measure of The Moon", The University of Chicago Press, (1963).

3. Bjork, R. L., Paper 1, Sixth Symposium on Hypervelocity Impact, Vol II, Part 1, (August, 1963).

4. Moore, Gault, Lugn and Shoemaker, Paper N, UCRL 6438, Part II, (October, 1961).

5. Bjork, R. L., Paper N, UCRL 6438, Part II, (October, 1961).

6. Walsh, J. M. and Tillotson, J. H., Paper 2, Sixth Symposium on Hypervelocity Impact, Vol II, Part 1, (August, 1963).

7. Maenchen, TENSOR, Lawrence Radiation Laboratory, UOPDFG1-1, (January, 1961).

8. Riney, "Visco-Plastic Solution of Hypervelocity Impact Cratering Phenomenon", Proc. Sixth Symposium on Hypervelocity Impact, Vol II, Part 1 (August, 1963).

9. Wilkins, "Calculation of Elastic-Plastic Flow", Lawrence Radiation Laboratory, UCRL 7322, (April, 1963).

10. Hamada, Harold, Symposium on the Equation of State for Earth Materials, AFSWC-TDR-62-126, (November, 1962).

11. "Static and Dynamic Behavior of a Playa Silt in One-Dimensional Compression", RTD TDR-63-3078, (September, 1963).

12. Bass, Hawk, and Chabai, "Hugoniot Data for Some Geologic Materials", SC-4903(RR) Sandia Corporation, (June, 1963).

13. Anderson, "Hugoniot Data on Moist Playa", S.R.I. private communication.

14. Bass, Hawk, Chabai, "Shock Hugoniots of Porous Earth Materials", paper delivered to 32nd International Meeting of The Society of Exploration Geophysicists, Calgary, Alberta, Canada, (September 20, 1962).

15. Chabai, "Synthesis of Shock Hugoniots forRock Materials", Proceedings of Fifth Symposium on Rock Mechanics, School of Mines and Metallurgy, Institute of Technology, University of Minnesota, Minneapolis, Pergamon Press Ltd, Oxford, England, (1962).

16. Lombard, "The Hugoniot Equation of State of Rocks", Lawrence Radiation Laboratory, Livermore, California, UCRL 6311, (February, 1961).

17. Ahrens, Gregson, Petersen, "Dynamic Properties of Rocks", AFCRL-63-662, Stanford Research Institute, (August 15, 1963).

18. McQueen, Marsh, "Equation of State of Nevada Alluvium", LAMS-2760, Los Alamos Scientific Laboratory, (November, 1961).

19. Bernstein and Keough, "Piezoresistivity of Manganin", S.R.I., private communication.

20. Grigorian, "Doklady", AN USSR 124, (1959) No. 2.

21. Grigorian, "Prikl, Mat, Mekh." 24 (1960) No. 6.

22. Grigorian, "Some Simplifications in the Description of the Motion of a Soft Soil", a paper given at the International Symposium on Stress Waves in Anelastic Solids, Brown University, (April 3-5, 1963).

23. Alexeenko, Grigorian, Novgorodov, Rykov; "Doklady" AN USSR 133 (1960) No. 6.

24. Alexeenko, Grigorian, Koshelev, Novgorodov, Rykov, "Prikl, Mat. Tekh, Fiz." (1963) No. 2.

25. Drucker, "Limit Analysis of Two and Three-Dimensional Soil Mechanics Problems", Journal Mech. and Physics of Solids, Vol. 1, 217 to 226, (1958).

26. Abhandlungen, aus dem Gebiete der technischen Mechanik, 2nd ed p. 192, W. Ernst und Sohn, Berlin, 1914; and Z. Ver. deut. Ing., Vol. 44, pp. 1524-1530; pp. 1572-1577; 1900; Vol. 45, p. 740, 1901.

27. Nuckolls, J. H., "A Computer Calculation of Rainier," Paper No. C-2 presented at the Second Plowshare Symposium, Lawrence Radiation Laboratory, Livermore, California, UCRL 5675, (May 15, 1959).

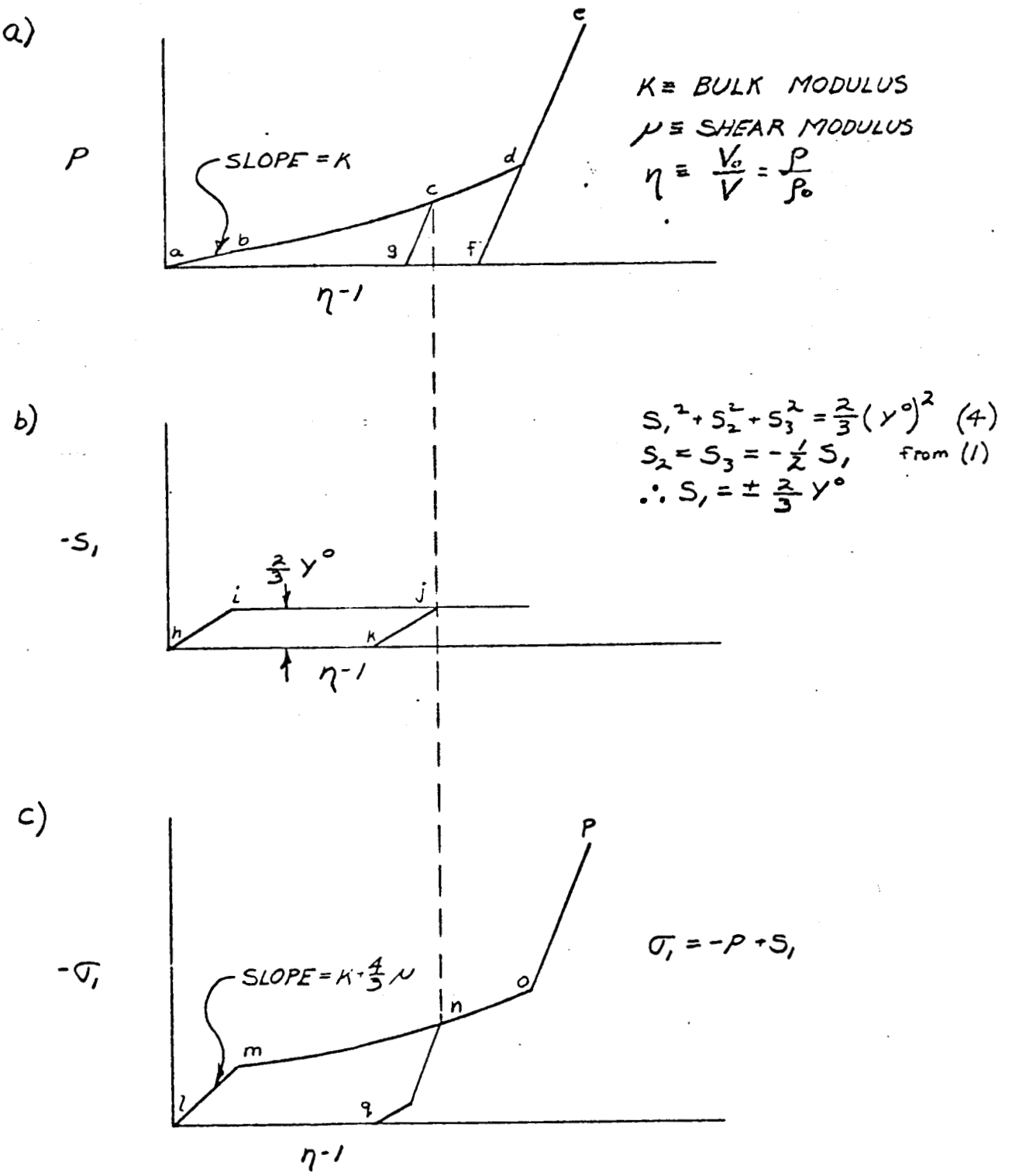

Figure 4.1 Von Mises Model

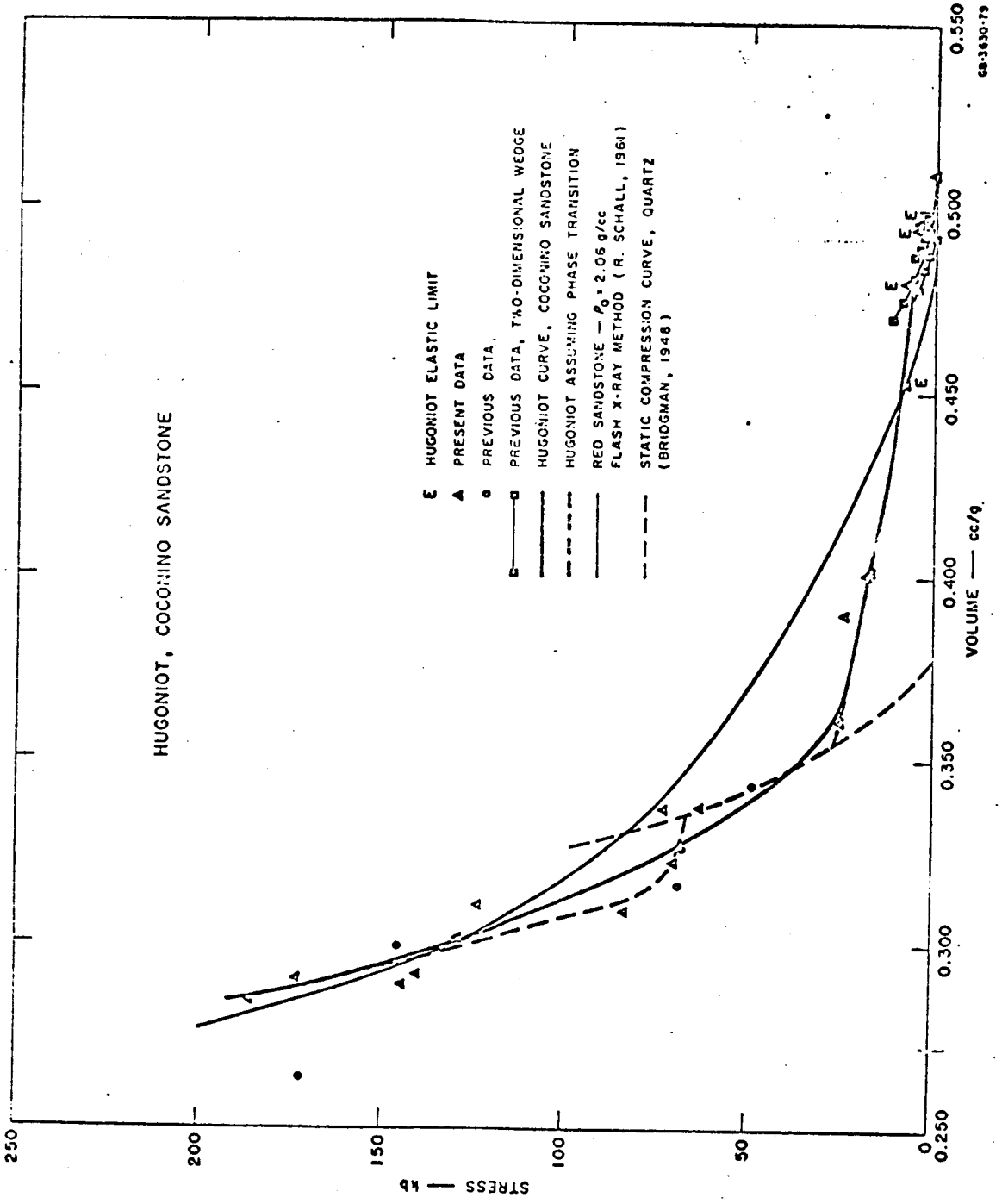

FIG. 4.2 HUGONIOT, SANDSTONE

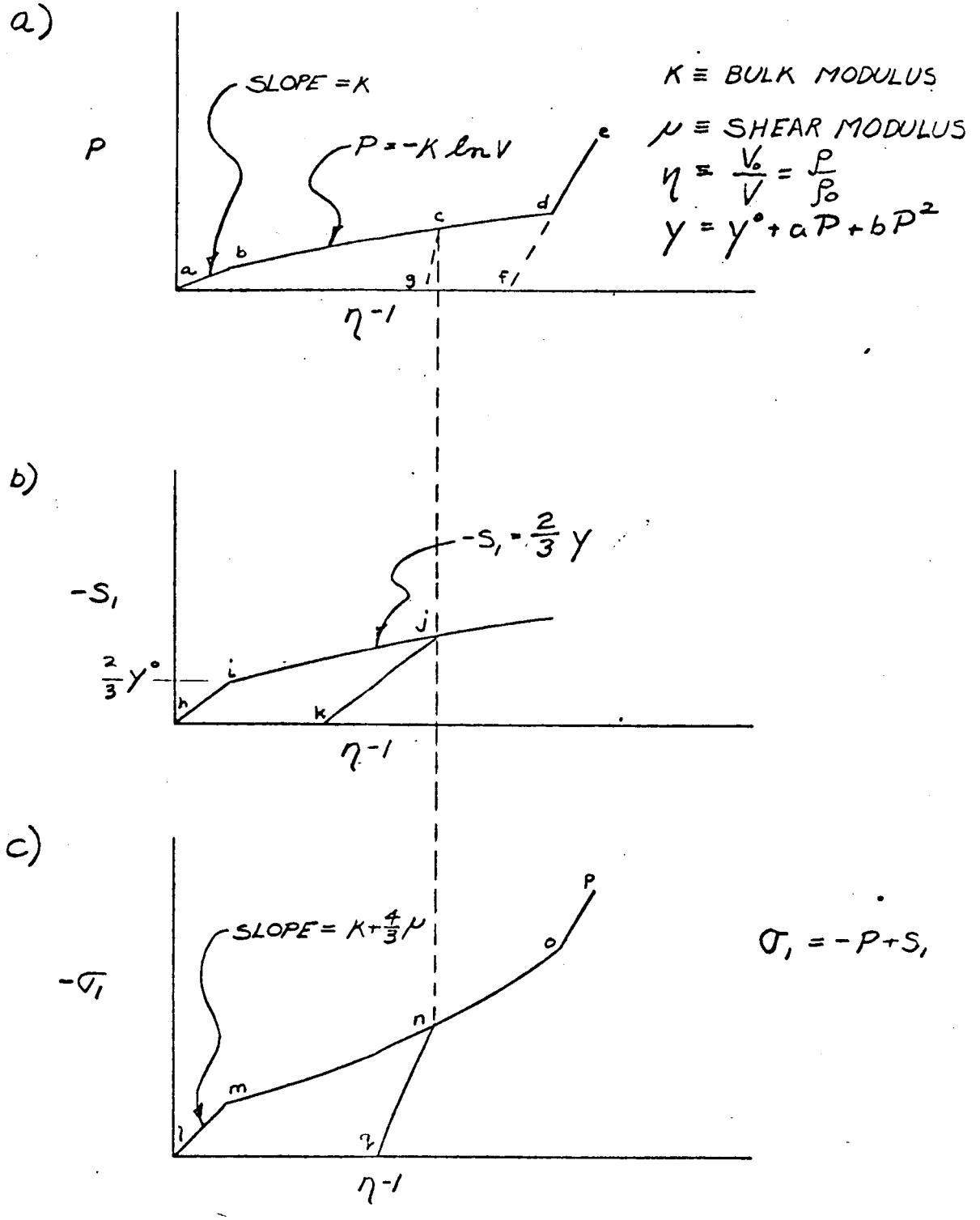

Figure 4.3 Coulomb Model

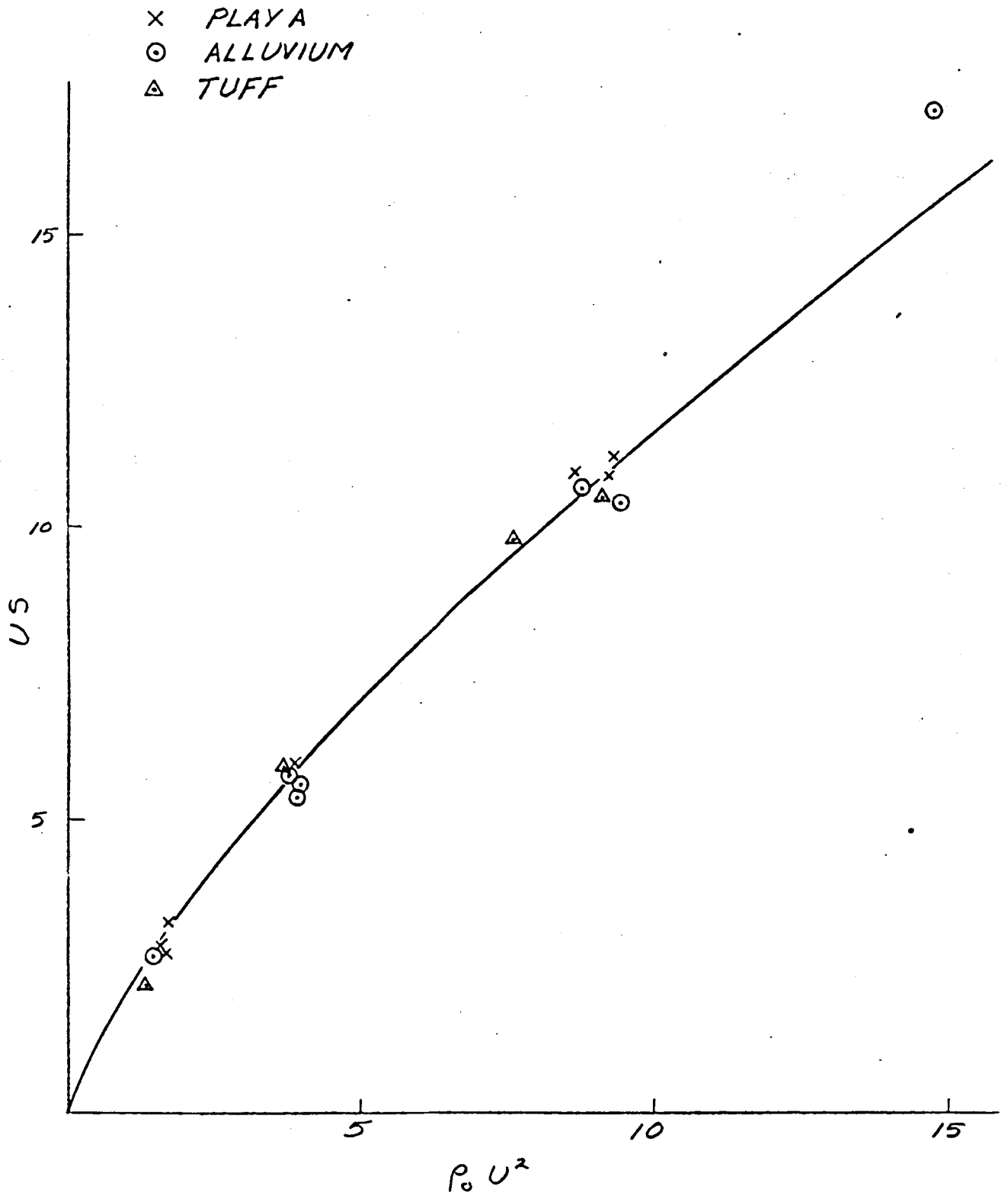

Figure 4.4

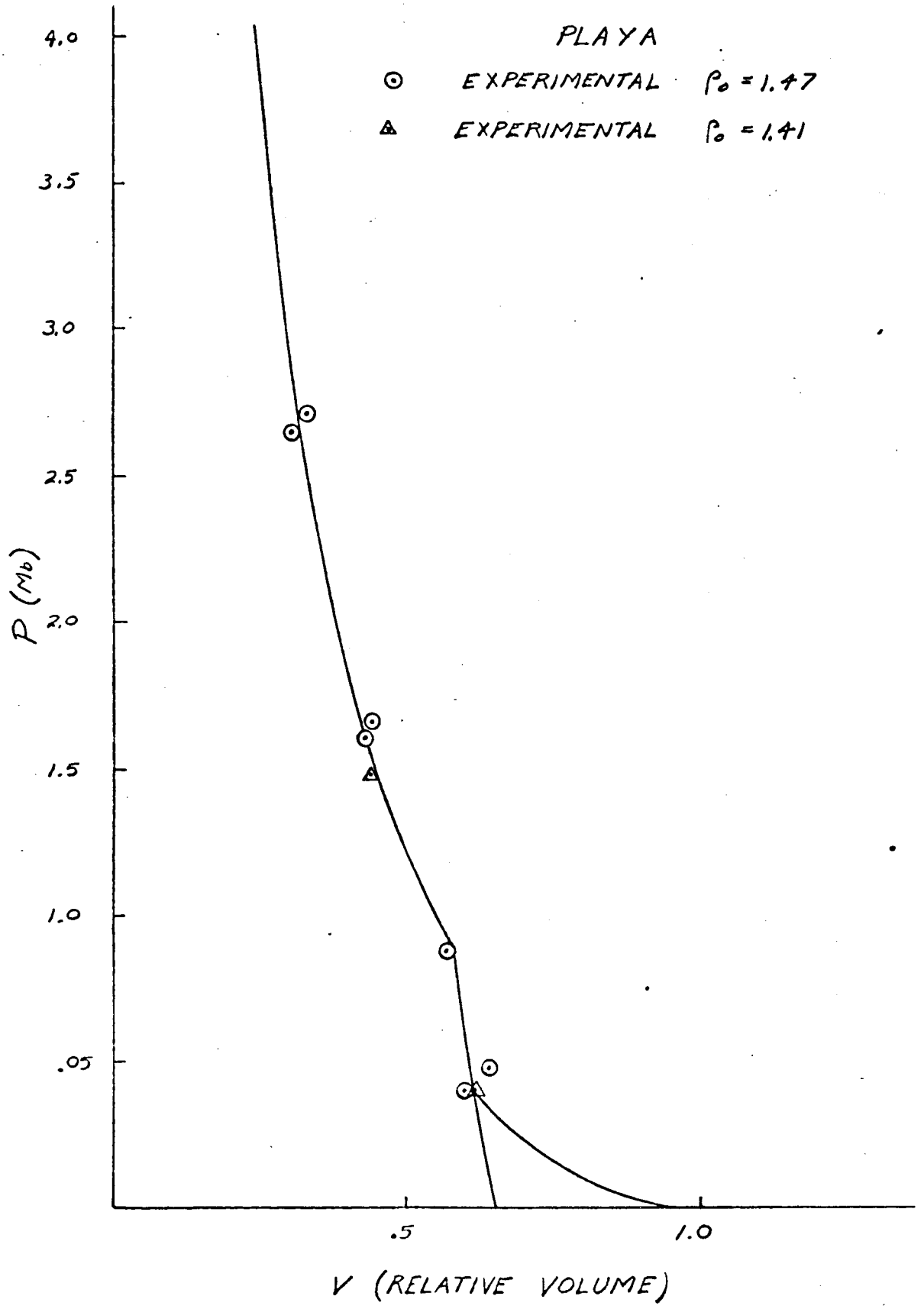
PLAYA
EXPERIMENTAL $\rho_o = 1.47$
EXPERIMENTAL $\rho_o = 1.41$
4.0
3.5
3.0
2.5
2.0
1.5
1.0
.05
P (Mb)
.5
1.0
V (RELATIVE VOLUME)

Figure 4.5

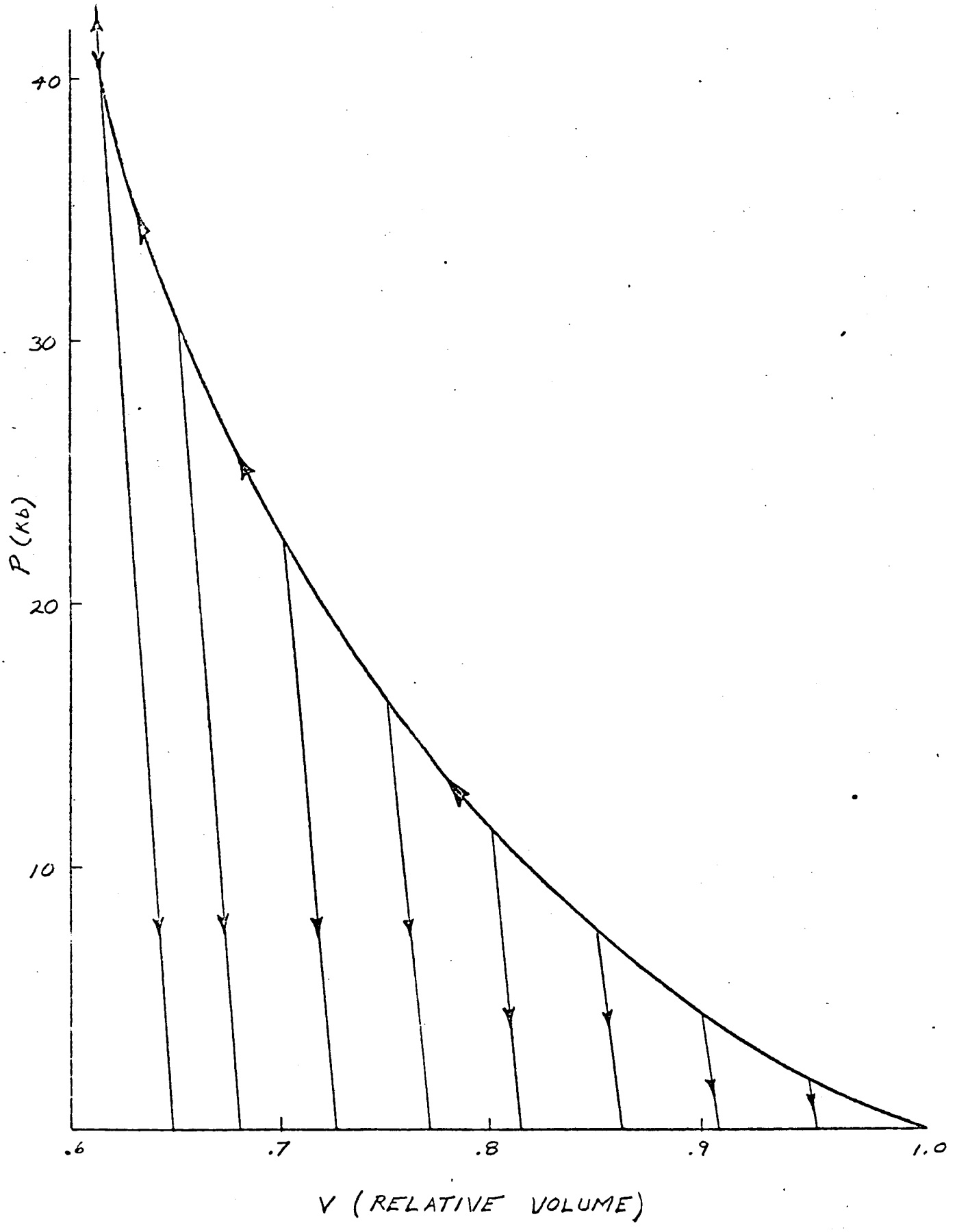

Figure 4.6

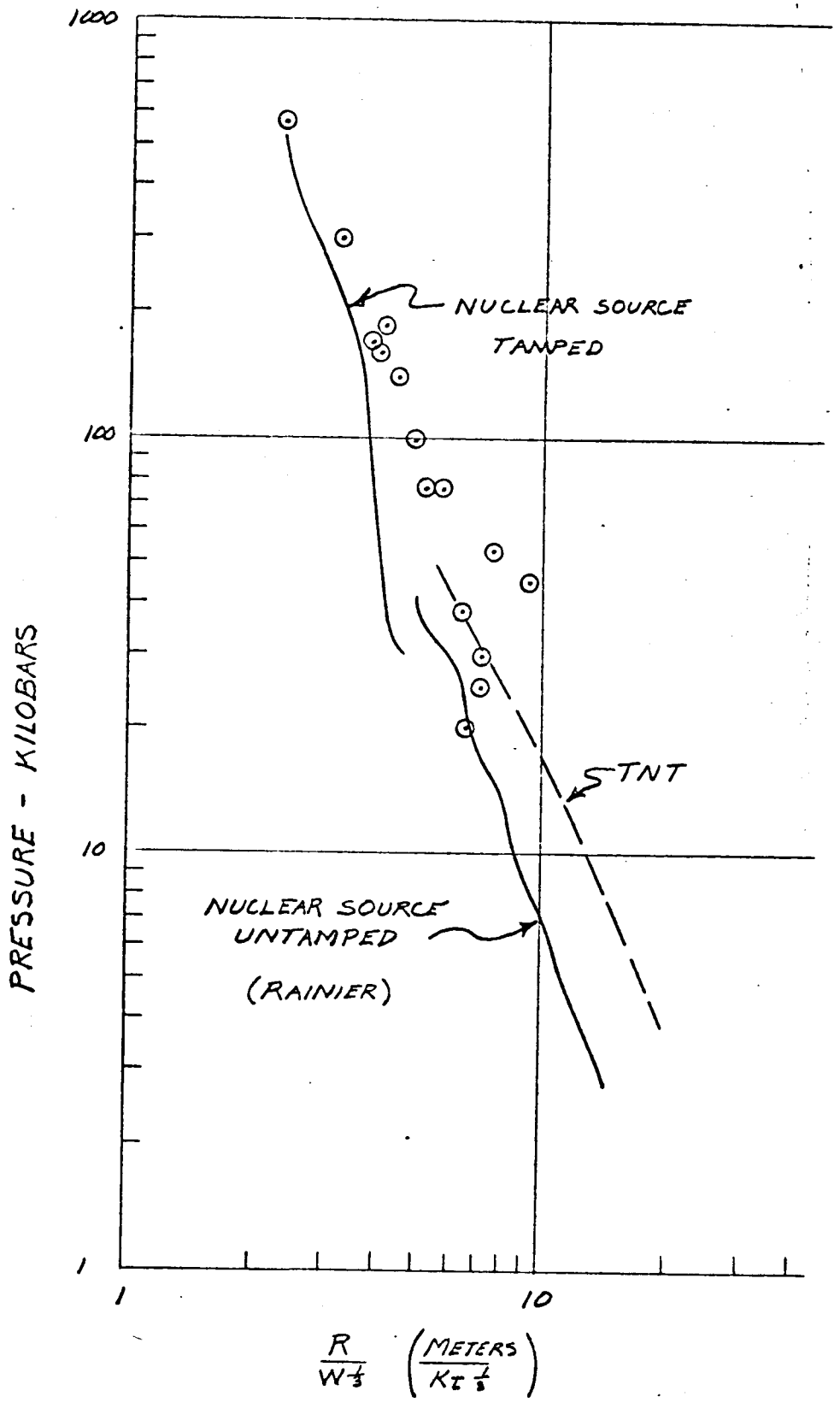
1000
100
10
1
PRESSURE - KILOBARS
NUCLEAR SOURCE
TAMPED
TNT
NUCLEAR SOURCE
UNTAMPED
(RAINIER)
1
10
R / W^1/3 (METERS / Kt^1/3)

Figure 5.1

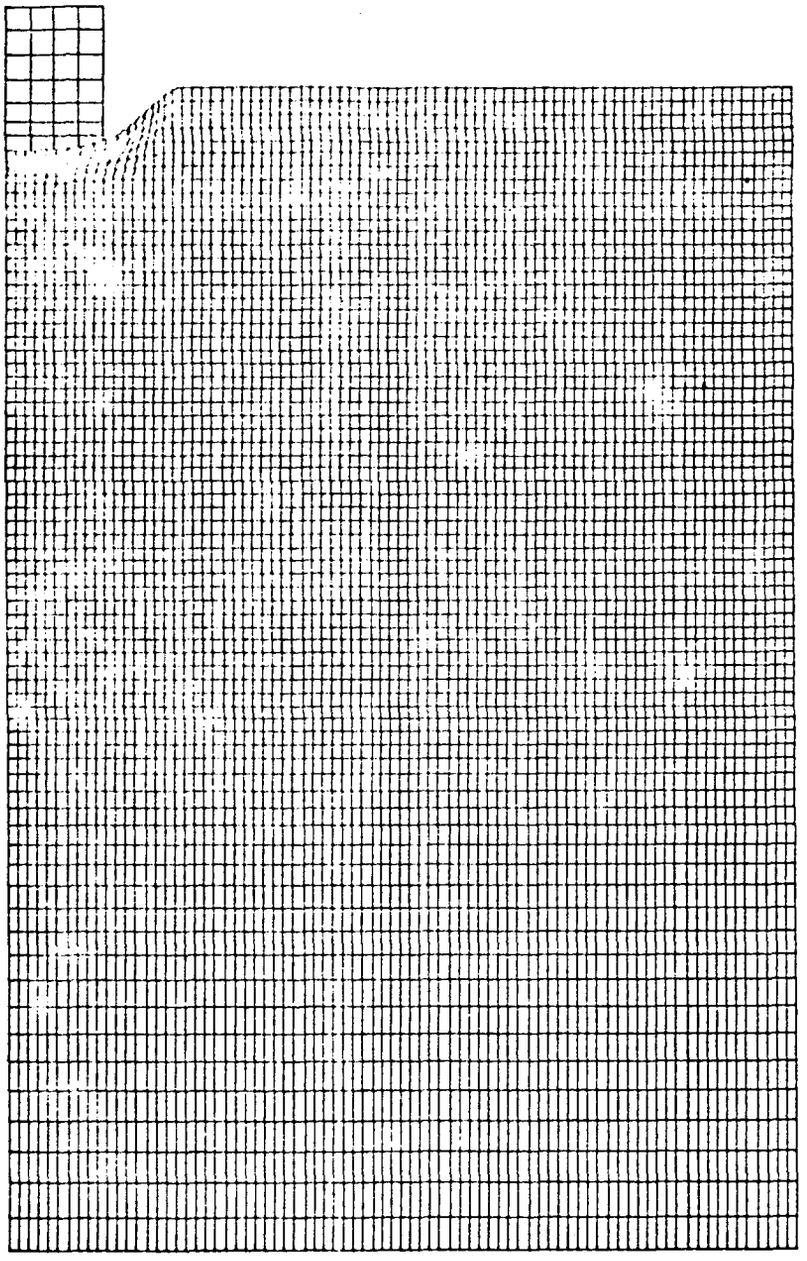

Figure 5.2

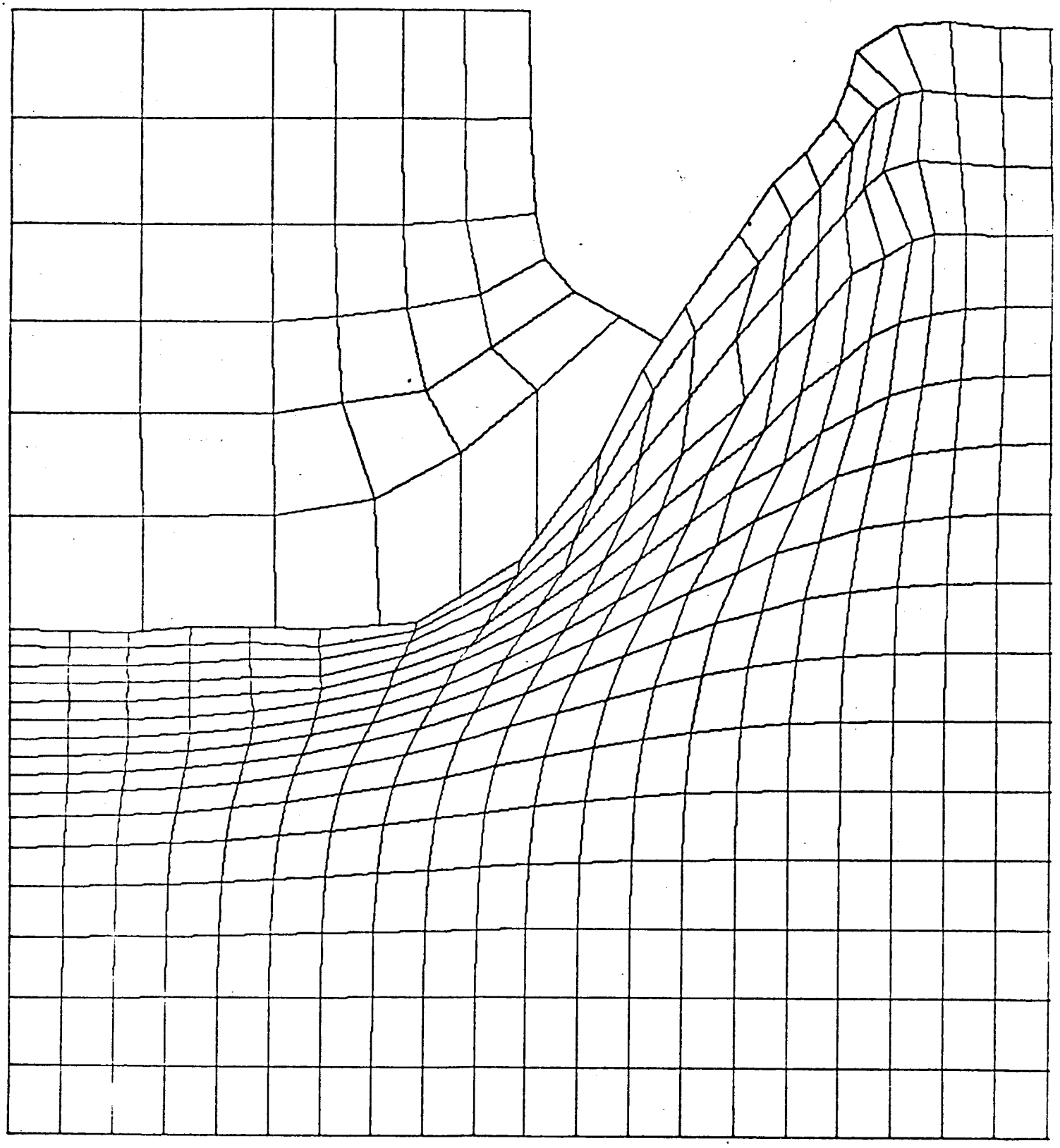

Figure 5.3

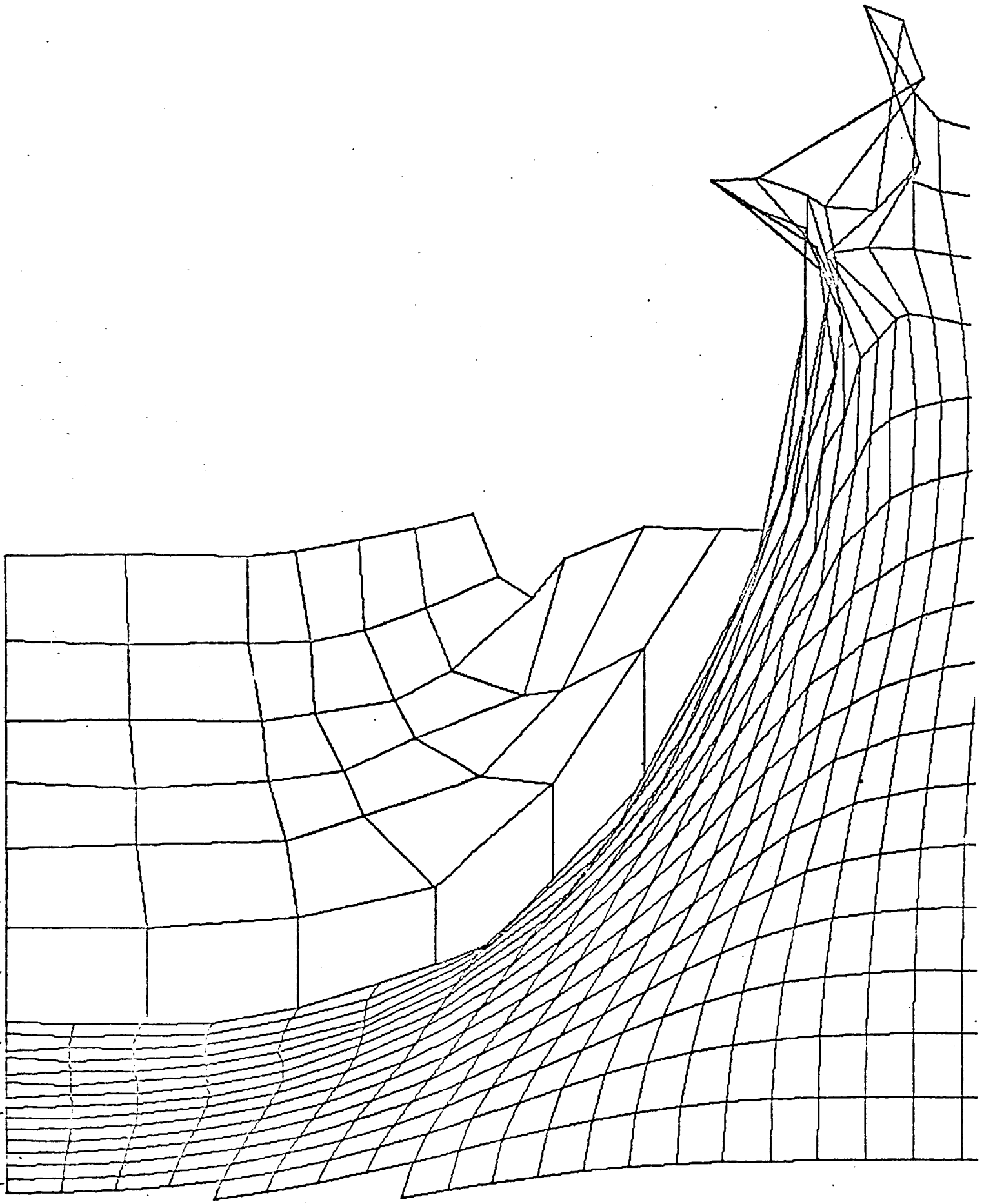

Figure 5.4

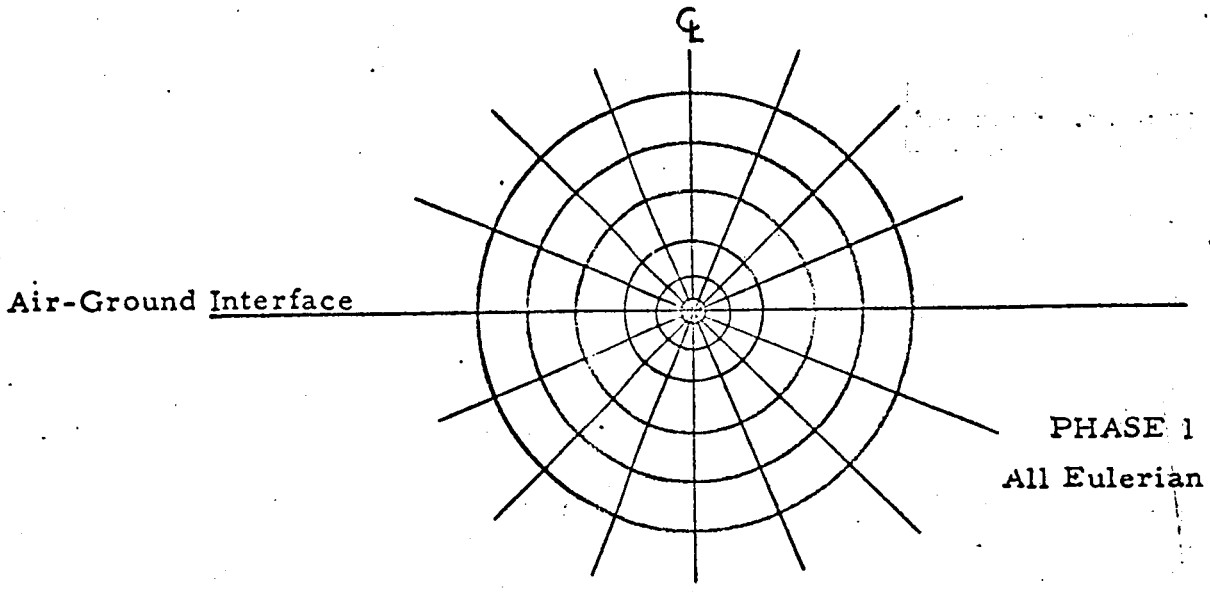

Figure 6.1a

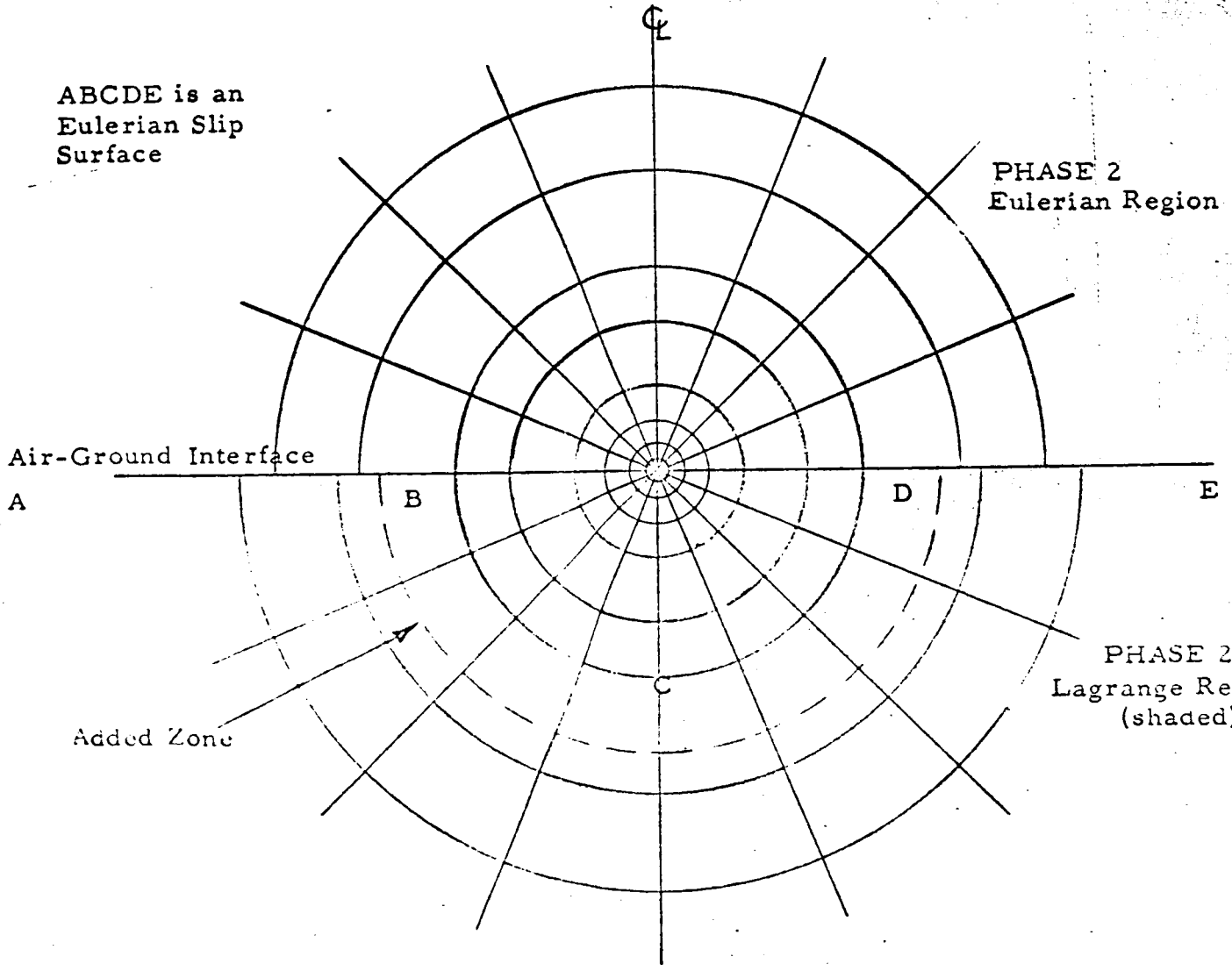

Figure 6.1b